

Direct inter-conduction-subband optical absorption of thin zinc-blende-structure-semiconductor rectangular wires

Johnson Lee and M. O. Vassell

GTE Laboratories Incorporated, 40 Sylvan Road, Waltham, Massachusetts 02254

(Received 18 December 1989; revised manuscript received 12 April 1990)

The optical absorption in direct-inter-conduction-subband transitions has been calculated in the electric-dipole approximation for a semiconducting thin wire fabricated from zinc-blende-structure material. Due to inversion asymmetry of the microscopic crystal potential, the 2×2 Hamiltonian in the spin- $\frac{1}{2}$ basis has nonvanishing off-diagonal elements. We have solved the equivalent matrix eigenvalue problem obtained by expanding the eigenvectors in an N -term double Fourier series chosen to satisfy the zero boundary conditions automatically. We have found that (1) the spin splittings are significant and are anisotropic depending on the magnitudes and orientations of the free-propagation wave vector, (2) the eigenvector is a mixture of spin states, and (3) the oscillator strengths are nonzero for the forbidden transitions. The optical-absorption spectrum for \hat{z} -polarized incident light with an energy $\hbar\omega$ is discussed.

I. INTRODUCTION

The spin splitting of the bands of zinc-blende-type semiconductors which possess inversion asymmetry has been known for a long time.¹⁻³ Christensen and Cardona⁴ have shown that the splitting of the spin degeneracy of the lowest conduction band of GaAs for \mathbf{k} along [110] is proportional to k^3 and has a maximum value of ≈ 75 meV. Evidently, the contributions of the k^3 terms in the conduction band for zinc-blende-type semiconductors are significant and are not negligible. Recently, Eppenga and Schuurmans⁵ calculated the splittings from a 2×2 Hamiltonian in the spin $s = \pm \frac{1}{2}$ basis including the inversion asymmetry of the microscopic crystal potential for GaAs/AlAs quantum wells [one-dimensional (1D) confinement]. They solved the eigenenergies of the Hamiltonian by adopting Nedorezov's method⁶ with appropriate boundary conditions, and found that the spin splitting of the conduction band is proportional to the wave vector k when \mathbf{k} is near the Brillouin-zone center, and is strongly anisotropic for quantum-well structures. We attempted to extend their technique to calculate the spin splittings of the conduction subbands of zinc-blende-type semiconductors in wire structures (2D confinement). However, we found that it was difficult to generalize Nedorezov's method because the eigenfunctions are no longer separable.

In this paper, we examine the effects of inversion asymmetry on GaAs quantum-wire structures using a different scheme. In Sec. II, a theoretical model is presented for calculating the eigenenergies and the corresponding eigenfunctions of the Hamiltonian, and then the direct-inter-subband optical absorption is discussed. In Sec. III, detailed numerical results of the spin splittings, oscillator strengths, and optical-absorption coefficient are reported. Finally, a summary is presented.

II. THEORETICAL MODEL

The Hamiltonian H describing the energy spectrum for the conduction band including the effects of the inversion asymmetry of the microscopic crystal potential is formulated in a spin $s = \pm \frac{1}{2}$ basis and is given in the atomic units by⁵

$$\underline{H} = \begin{pmatrix} H_{11} & H_{12} \\ H_{12}^* & H_{22} \end{pmatrix}, \quad (1)$$

$$H_{11} = (k_x^2 + k_y^2 + k_z^2)/m^* + \frac{1}{2}\gamma k_z [(k_x^2 - k_y^2)\cos^2\varphi - 2k_x k_y \sin(2\varphi)], \quad (2)$$

$$H_{22} = (k_x^2 + k_y^2 + k_z^2)/m^* - \frac{1}{2}\gamma k_z [(k_x^2 - k_y^2)\cos^2\varphi - 2k_x k_y \sin(2\varphi)], \quad (3)$$

$$H_{12} = \frac{1}{2}\gamma \{ k_z^2 (k_x + ik_y) e^{i\varphi} - \frac{1}{2}i [(k_x^2 - k_y^2)\sin(2\varphi) + 2k_x k_y \cos(2\varphi)] (k_x - ik_y) e^{-i\varphi} \}, \quad (4)$$

where the conduction-band edge is chosen to be zero, m^* is the Γ -point conduction-band effective mass, γ is the spin-splitting parameter, $\mathbf{k} = (k_x, k_y, k_z)$ is the wave vector, and φ is the angle between k_x and [100]. Here k_x and k_y are assumed to be in [100] and [010] plane as indicated in the inset of Fig. 1. We consider a thin rectangular GaAs wire with cross-sectional dimensions L_y and L_z along \hat{y} and \hat{z} , respectively. The electron motion is free in the longitudinal direction \hat{x} , but is completely confined in the transverse direction (\hat{y}, \hat{z}) by a 2D infinite potential well. In order to evaluate the conduction subbands, we treat k_x as a continuum and replace k_y and k_z by $-i \partial_y$

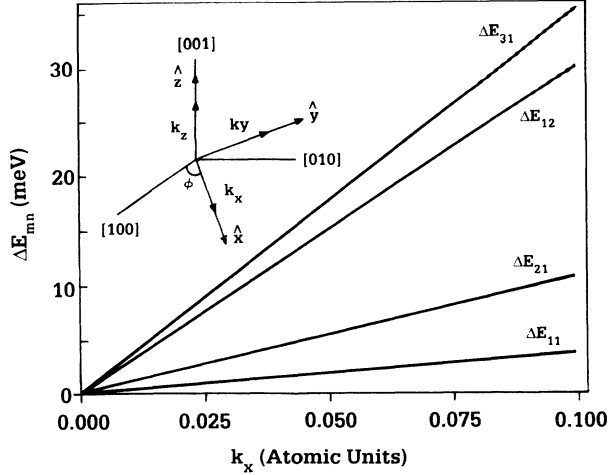


FIG. 1. The spins splittings ΔE_{mn} vs k_x for $\varphi=0$. The inset shows the definitions of crystal orientations $[i j k]$, wave vector (k_x, k_y, k_z) and quantum wire's directions $(\hat{x}, \hat{y}, \hat{z})$.

and $-i \partial z$, respectively. We wish to solve the Schrödinger equation

$$\underline{H} \begin{bmatrix} \psi_1(x, y, z) \\ \psi_2(x, y, z) \end{bmatrix} = E \begin{bmatrix} \psi_1(x, y, z) \\ \psi_2(x, y, z) \end{bmatrix} \quad (5)$$

plus the boundary conditions

$$\begin{aligned} \psi_j(x, 0, z) &= \psi_j(x, L_y, z) = \psi_j(x, y, 0) \\ &= \psi_j(x, y, L_z) = 0, \quad j = 1, 2. \end{aligned}$$

Examination of Eqs. (2)–(4) shows that operators, H_{11} , H_{22} , and H_{12} contain first-, second-, and third-order derivatives with respect to y or z . If we adopt Nedorezov's method⁶ and choose the trial wave function as

$$\psi_j(x, y, z) = e^{ik_x x} \sum_{k_y, k_z} A_j(k_y, k_z) e^{i(k_y y + k_z z)}$$

the secular equation has the form

$$f(k_x, k_y, k_z; E) = 0,$$

which correlates k_y as a function of $(k_x, k_z; E)$. The zero boundary conditions are then given by

$$\begin{aligned} \sum_{k_y, k_z} A_j(k_y, k_z) e^{ik_z z} &= \sum_{k_y, k_z} A_j(k_y, k_z) e^{i(k_y L_y + k_z z)} \\ &= \sum_{k_y, k_z} A_j(k_y, k_z) e^{ik_y y} \\ &= \sum_{k_y, k_z} A_j(k_y, k_z) e^{i(k_y y + k_z L_z)} = 0, \end{aligned}$$

where A_j are unknowns. We notice that the zero boundary conditions apparently include the y and z dependences. Similar difficulties have been encountered by Suemune and Coldren⁷ when they studied the Kohn-Luttinger Hamiltonian for the valence subbands in quantum-wire structures. They argued that by assuming various y and z values, the valence subband structures can be obtained numerically and are independent of the assigned y and z values. However, they did not give any mathematical proof, and we believe that the proof may not be easy. Therefore, we seek a different numerical scheme to solve the problem.

In order to satisfy the zero boundary conditions automatically, we chose the eigenvector to be

$$\begin{aligned} \psi_j(x, y, z) &= e^{ik_x x} \left[\frac{4}{L_y L_z} \right]^{1/2} \\ &\times \sum_{k, l=1}^{\infty} a_{kl}^{(j)} \sin \left[\frac{k \pi y}{L_y} \right] \sin \left[\frac{l \pi z}{L_z} \right], \\ & \quad j = 1, 2, \quad (6) \end{aligned}$$

where $a_{kl}^{(j)}$ are unknowns. A straightforward manipulation after substituting Eq. (6) into Eq. (5) gives the complicated set of coupled equations,

$$\begin{aligned} \alpha_{mn} a_{mn} + p_{mn} b_{mn} - i \sum_{k, l=1}^{\infty} q_{kl}(m, n) a_{kl} \\ + \sum_{k, l=1}^{\infty} s_{kl}(m, n) b_{kl} = E a_{mn}, \quad (7) \end{aligned}$$

$$\begin{aligned} \alpha_{mn} b_{mn} + p_{mn}^* a_{mn} + i \sum_{k, l=1}^{\infty} q_{kl}(m, n) b_{kl} \\ - \sum_{k, l=1}^{\infty} s_{kl}^*(m, n) a_{kl} = E b_{mn}, \quad (8) \end{aligned}$$

where

$$\begin{aligned} a_{mn}^{(1)} &= a_{mn}, \quad a_{mn}^{(2)} = b_{mn}, \\ \alpha_{mn} &= \frac{1}{m^*} \left[k_x^2 + \left[\frac{m \pi}{L_y} \right]^2 + \left[\frac{n \pi}{L_z} \right]^2 \right], \\ p_{mn} &= \frac{k_x \gamma}{2} \left[\left[\frac{n \pi}{L_z} \right]^2 e^{i\varphi} - \frac{1}{2} i e^{-i\varphi} \left\{ \left[k_x^2 - \left[\frac{m \pi}{L_y} \right]^2 \right] \sin(2\varphi) - 2i \left[\frac{m \pi}{L_y} \right]^2 \cos(2\varphi) \right\} \right], \\ q_{kl}(m, n) &= \frac{\gamma}{2} \left[(l \pi / L_z) I_z(n, l) \left\{ \left[k_x^2 - \left[\frac{k \pi}{L_y} \right]^2 \right] \cos(2\varphi) \delta_{m, k} + 2i k_x \frac{k \pi}{L_y} \sin(2\varphi) I_y(m, k) \right\} \right], \end{aligned}$$

and

$$s_{kl}(m, n) = \frac{\gamma}{2} \frac{k\pi}{L_y} I_y(m, k) \delta_{n,l} \left[(l\pi/L_z)^2 e^{i\varphi} + \frac{1}{2} i e^{-i\varphi} \left\{ \left[k_x^2 - \left(\frac{k\pi}{L_y} \right)^2 \right] \sin(2\varphi) + 2ik_x^2 \cos(2\varphi) \right\} \right],$$

with

$$I_j(s, t) = \begin{cases} \frac{1}{\pi} \left[\frac{1 - (-1)^{s-t}}{s-t} + \frac{1 - (-1)^{s+t}}{s+t} \right] & \text{if } s \neq t \\ 0 & \text{if } s = t. \end{cases}$$

Here, s, t, k, l, m , and n are integers; $j = y$ or z . If we assume that k, l, m , and n have a finite range from 1 to N , where N is an arbitrary integer, Eqs. (7) and (8) can be cast into a matrix with a dimension of $2N^2$. Therefore, the problem becomes a typical matrix eigenvalue calculation. By increasing N step by step, we examine the convergence of the eigenenergies until a preset criterion is met. As a guideline for our numerical manipulations, we perform a degenerate perturbation calculation. We treat H_{12} as a small perturbation and evaluate the first-order correction. The results are surprisingly simple and are given by

$$E_{mn} = \alpha_{mn} \pm \Delta\alpha_{mn} \quad (9)$$

with

$$\Delta\alpha_{mn} = \left| \frac{\gamma k_x}{2} \right| \left\{ \left[\left(\frac{n\pi}{L_z} \right)^2 - \left(\frac{m\pi}{L_y} \right)^2 \right]^2 \cos^2(2\varphi) + \left[k_x^2 - \left(\frac{m\pi}{L_y} \right)^2 - \left(\frac{n\pi}{L_z} \right)^2 \right]^2 \sin^2(2\varphi) \right\}^{1/2},$$

where α_{mn} has been defined in Eqs. (7) and (8). Therefore, the spin splittings due to the inversion asymmetry are $\Delta E_{mn} = 2\Delta\alpha_{mn}$. Once the eigenenergies and the corresponding eigenvectors are determined, we proceed to investigate the direct-inter-subband absorption.

The linear response of a thin quantum-wire structure to a light wave is calculated by a conventional procedure⁸ and was discussed in detail in Ref. 9. The optical absorption due to direct-inter-subband transitions and including broadening effects can be obtained by using an electric-dipole approximation. When the electromagnetic wave is polarized along the \hat{z} axis, a direction of size quantization in the thin wire, the conductivity tensor in \hat{z} can be written as⁹

$$\sigma_{33} = \frac{i}{m^* \omega \Omega} \sum_{\alpha, \alpha', s} \omega_{\alpha'\alpha} O_{\alpha'\alpha} f_0(E_\alpha) [1 - f_0(E_{\alpha'})] \times \left[\frac{1}{\omega - \omega_{\alpha'\alpha} + i\Gamma} - \frac{1}{\omega - \omega_{\alpha'\alpha} - i\Gamma} \right], \quad (10)$$

where the following abbreviations have been adopted:

$$\hbar\omega_{\alpha'\alpha} = E_{\alpha'} - E_\alpha,$$

$$O_{\alpha'\alpha} = \frac{4}{m^* \omega_{\alpha'\alpha}} |(\alpha | \partial_z | \alpha')|^2$$

is the oscillator strength; and $f_0(E_\alpha)$ is the Fermi-Dirac distribution function. Here, s denotes electron spin states, Γ is the half-width due to collisions, and $|\alpha\rangle = |k_x; m, n, \sigma\rangle$ [$|\alpha'\rangle$] is the initial (final) state. The symbol $\sigma = \pm$ is used to indicate the spin splittings (increase or decrease from α_{mn}). Note that since k_x is a continuum,

an integration over k_x from $-\infty$ to $+\infty$ must be performed to obtain σ_{33} in Eq. (10). Since σ_{33} is complex, so is the dielectric function, i.e., $\epsilon = \epsilon_1 + i\epsilon_2$. The relation between σ_{33} and ϵ is given by

$$\epsilon_1 = \epsilon_b - 4\pi \text{Im}(\sigma_{33})/\omega,$$

and

$$\epsilon_2 = 4\pi \text{Re}(\sigma_{33})/\omega,$$

where ϵ_b is the bulk dielectric constant (=13.18 for GaAs). The optical-absorption coefficient η_{33} and the index of refraction \bar{n} are obtained as

$$\bar{n} = \{[\epsilon_1^2 + (\epsilon_2^2 + \epsilon_2^2)^{1/2}]/2\}^{1/2}$$

and

$$\eta_{33} = 4\pi \text{Re}(\sigma_{33})/\bar{n}c,$$

where c is the speed of light.

Before we end this section, we discuss some of the implications of our model. The wave function defined by Eq. (6) indicates that when the inversion asymmetry of the semiconductor exists, i.e., γ is not negligible, the wave function ψ_j must be a mixture of various eigenmodes of $\sin(k\pi y/L_y)$ and $\sin(l\pi z/L_z)$ because H_{12} in Eq. (1) is nonzero. A direct consequence of the mixing of the spin states is the spin splittings of the conduction subbands as approximated and shown in Eq. (9). The spin splittings are expected to be anisotropic in φ . The conductivity in Eq. (10) implies that when \hat{z} -polarized light with an energy $\hbar\omega \cong \hbar\omega_{\alpha'\alpha}$ can be absorbed by the wire, i.e., when the transition has a nonzero oscillator strength, a strong resonance peak with a half-width Γ is expected to show in the real part of $\sigma_{33}(\omega)$. This kind of resonance must also be reflected in the absorption coefficient be-

cause η_{33} is proportional to $\text{Re}(\sigma_{33})$ and \bar{n} is a slow varying function of ω .

III. NUMERICAL RESULT AND DISCUSSION

In order to perform the numerical calculations for GaAs quantum-wire structures, we chose $L_y=80$ Å, $L_z=60$ Å, $m^*/m_0=0.067$, and $\gamma=17$ eV Å³.⁵ We solve the coupled equations [Eqs. (7) and (8)] with $k_x=0.01$ a.u. and $\varphi=\pi/4$ by increasing N step by step to see how fast the eigenenergies converge. We show the results in Table I. Notice that the eigenenergies have converged already to the fourth significant figure by order $N=4$. The last row in Table I shows that when γ is zero, i.e., the crystal has inversion symmetry, the eigenenergies become degenerate [$E_1=E_2=\alpha_{11}$, $E_3=E_4=\alpha_{21}$, $E_5=E_6=\alpha_{12}$, and $E_7=E_8=\alpha_{31}$; α_{mn} is defined in Eqs. (7) and (8)]. Usually, for a Ga_{1-x}Al_xAs/GaAs quantum well, the potential barrier V_e is about 300 meV; thus, those $E_n(k_x=0)$ larger than V_e become unrealistic, and a finite-potential-barrier model must be used. Here, we limit our model to an infinite potential well. In the discussions to follow, we take $N=4$, which yields a matrix with a dimension of 32×32 to demonstrate our numerical results. The spin splittings are defined as $\Delta E_{11}=E_2-E_1$, $\Delta E_{21}=E_4-E_3$, $\Delta E_{12}=E_6-E_5$, and $\Delta E_{31}=E_8-E_7$ (see Table I). First, we examine the energy splittings ΔE_{mn} as a function of k_x when k_x is parallel to [100] (i.e., $\varphi=0$), and show the results in Fig. 1. The inset figure is used to indicate the relation between crystal axes and (k_x, k_y, k_z) together with (x, y, z) . Here, we see that the spin splittings ΔE_{mn} are linear functions of k_x , exactly as predicted by degenerate perturbation theory [see Eq. (9)]. However, if φ is $\pi/4$, i.e., k_x is along [110], the variations of ΔE_{mn} with k_x are N shaped as shown in Fig. 2. By setting $\varphi=\pi/4$, Eq. (9), we have

$$\Delta E_{mn} = \left| \left[\frac{\gamma k_x}{2} \right] \left[k_x^2 - \left[\frac{m\pi}{L_y} \right]^2 - \left[\frac{n\pi}{L_z} \right]^2 \right] \right| \quad (13)$$

indicating that ΔE_{mn} as a function of k_x have two zeros. This explains why our numerical results have N -shaped plots. In Fig. 3(a), we plot the variations of ΔE_m versus φ with k_x fixed at 0.05 a.u., and in Fig. 3(b), we show the variation of ΔE_{mn} in polar coordinates ($\rho=\Delta E_{mn}$, φ) with $\Delta E_x=\Delta E_{mn} \cos\varphi$ and $\Delta E_y=\Delta E_{mn} \sin\varphi$. We see clearly that ΔE_{mn} have $4mm$ symmetry. Again, this re-

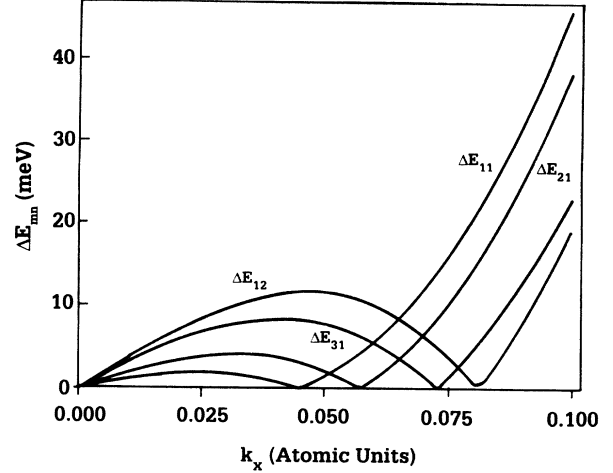


FIG. 2. The spin splittings ΔE_{mn} vs k_x for $\varphi=\pi/4$.

sult is exactly predicted by Eq. (9). We may conclude that the variations of the spin splittings ΔE_{mn} can be well approximated by first-order degenerate perturbation theory within 5% because of the smallness of γ ($=17$ eV Å³ for GaAs).

In our numerical scheme, we define the probability densities as $\rho_j=|\psi_j(x,y,z)|^2$, and $\int \int \int (\rho_1 + \rho_2) dx dy dz = 1$ to ensure the wave functions are normalized. By employing the results for E_{mn} and ψ_j provided above, we proceed to evaluate the absorption coefficient η_{33} and the index of refraction \bar{n} as shown in Eq. (12). The following parameters were chosen for numerical calculations: $\varphi=0^\circ$, $\Gamma=2$ meV, and $k_B T=6.64$ meV ($=77$ K). We assume that the Fermi energy lies above the ground-state energy E_{11} at zone center by 20 meV; thus, all electrons populate only the ground state because the energy differences between the excited states and the ground state are much larger than $k_B T$. For \hat{z} -polarized incident light, the oscillator strengths $O_{\alpha'\alpha}$ are plotted in Fig. 4 as a function of k_x . The initial state is $|\alpha\rangle=|1,1,-\rangle$ and the final state is $|\alpha'\rangle=|m,n,\sigma\rangle$ with k_x omitted. Here, we notice that for each pair of $|m,n,+\rangle$ and $|m,n,-\rangle$ states, only one of them has significant oscillator strength. Therefore, with m and n fixed, only one of the spin-splitting states, either $\sigma=+$ or $\sigma=-$, can be revealed in the absorption spectrum. When a \hat{z} -polarized light with an energy $\hbar\omega$ is absorbed

TABLE I. Eigenenergies [E_j (meV), $j=1-8$] of a quantum wire with parameters: $L_y=80$ Å, $L_z=60$ Å, $m^*/m_0=0.067$, $\gamma=17$ eV Å³, $k_x=0.01$ a.u., and $\varphi=\pi/4$. $2N^2$ is the dimension of the matrix to be solved. The last row shows α_{mn} (meV) for the case of $\gamma=0$.

N	E_1 (meV)	E_2 (meV)	E_3 (meV)	E_4 (meV)	E_5 (meV)	E_6 (meV)	E_7 (meV)	E_8 (meV)
2	263.367 13	264.438 21	526.077 89	527.892 06	729.725 91	733.438 37	996.943 51	
4	263.367 29	264.438 37	526.076 64	527.890 80	729.725 23	733.437 68	963.876 17	966.921 94
6	263.367 37	264.438 45	526.076 51	527.890 67	729.725 40	733.437 93	963.872 68	966.918 43
	α_{11}		α_{21}		α_{12}		α_{31}	
	263.902 87		526.986 19		731.606 55		965.458 39	

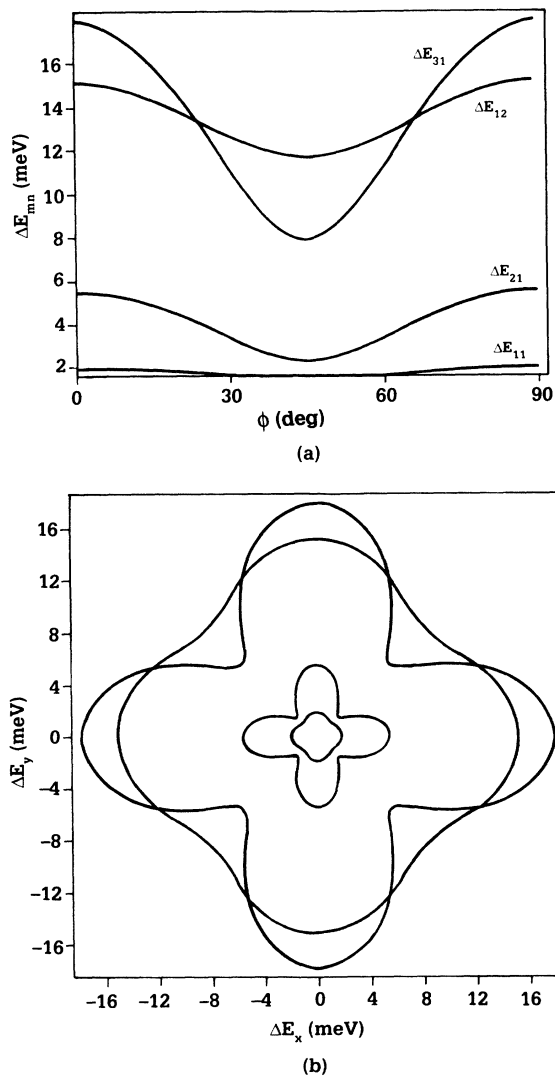


FIG. 3. (a) The variations of the spin splittings ΔE_{mn} with φ ; (b) same as (a) but plotted in polar coordinates [$\rho = \Delta E_{mn}$, φ]. In both plots, $k_x = 0.05$ a.u.

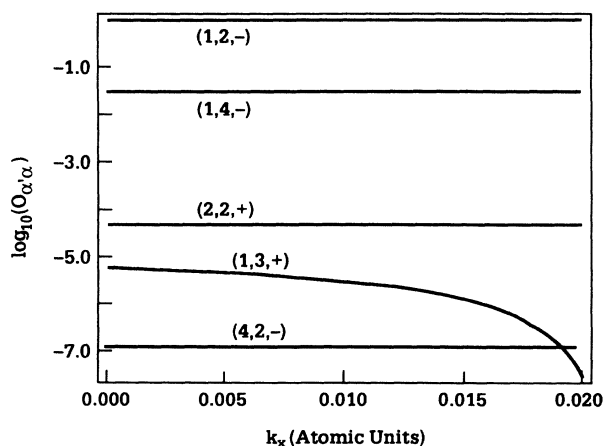


FIG. 4. The variations of the oscillator strengths $O_{\alpha\alpha}$ with k_x . The transition state is indicated by (m, n, σ) .

by the wire, the variations of the index of refraction \bar{n} and the optical-absorption coefficient η_{33} with the normalized photon energy $\hbar\omega/E_z^0$ (with $E_z^0 = \pi^2/m^*L_z^2$) are shown in Figs. 5(a) and 5(b), respectively. From both figures, we notice that resonances occur when $\hbar\omega/E_z^0$ is near 3, 4.7, 8, 11.4, and 15. These resonances can be explained by the following simple argument. If γ is zero, $\hbar\omega_{\alpha\alpha}$ is given by

$$\frac{\hbar\omega_{\alpha\alpha}}{E_z^0} = \frac{(m^2 - 1)L_z^2}{L_y^2} + (n^2 - 1). \quad (14)$$

The oscillator strength with $\gamma = 0$ yields a selection rule which requires that (i) the quantization state along \hat{y} be identical, i.e., $m = 1$, and (ii) the final state along \hat{z} be even integers, i.e., $n = 2, 4, 6, \dots$. Therefore, $\hbar\omega_{\alpha\alpha}/E_z^0$ equals $n^2 - 1$ and yields 3 and 15 with $n = 2$ and 4, respectively. All other transitions are forbidden because the corresponding oscillator strengths are zero. However, when γ is nonzero, the eigenvector is a mixture of the spin states and the so-called forbidden transitions now have nonzero oscillator strengths as discussed earlier in Fig. 4. These forbidden transitions are identified as $(2, 2, +)$, $(1, 3, +)$,

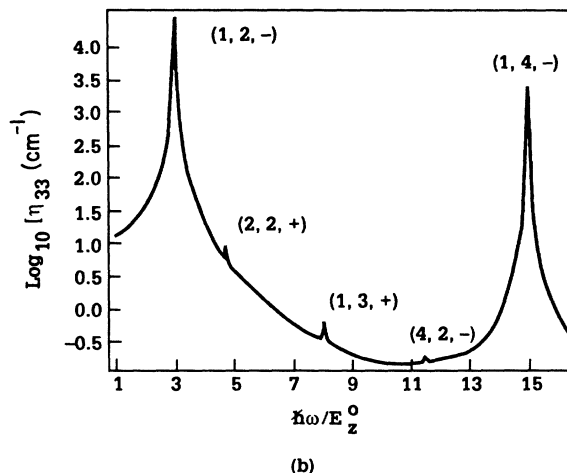
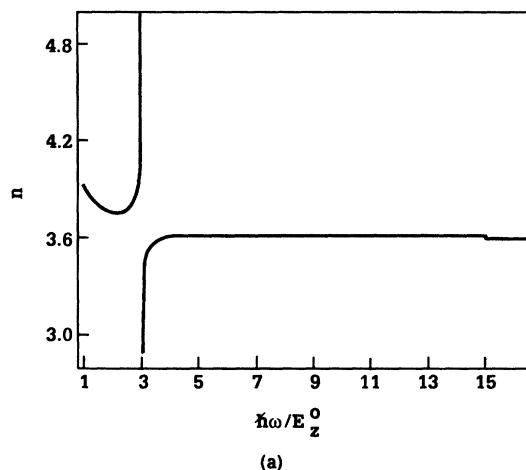


FIG. 5. The variation of (a) the index of refraction and (b) the absorption coefficient with $\hbar\omega/E_z^0$ for $\varphi = 0$.

and $(4, 2, -)$ and are revealed in the absorption spectrum as indicated in Fig. 5. The energy locations of these small peaks can also be approximated by Eq. (14).

IV. SUMMARY

We have studied the direct-inter-conduction-subband optical absorption of semiconducting thin wire of zincblende-type material which possesses the inversion asymmetry of the microscopic crystal potential. The inversion asymmetry of the microscopic crystal potential is seen to cause spin splitting of the conduction subbands. The splittings were calculated from a 2×2 Hamiltonian matrix, which contains nonzero off-diagonal elements in the spin $\pm \frac{1}{2}$ basis. By using an N -term Fourier series expansion

for the wave functions chosen to satisfy zero boundary conditions, we transformed the Schrödinger equation into a $2N^2 \times 2N^2$ matrix eigenvalue problem that could be solved accurately. Our numerical results indicated that, compared with results for diamond structure, (1) the spin splittings are significant and anisotropic for certain magnitudes and orientations of the free-propagation wave vector and (2) the eigenvectors are distorted because of the mixture of the spin states and the oscillator strengths are nonzero for the forbidden transitions. From the computed eigenenergies and eigenvectors, we investigated the index of refraction and the absorption coefficient within the electric-dipole approximation. When a \hat{z} -polarized incident light with energy $\hbar\omega$ is absorbed by the thin wire, resonance phenomena were predicted at $\hbar\omega \propto (m^2 - 1)L_z^2/L_y^2 + (n^2 - 1)$.

¹G. Dresselhaus, Phys. Rev. **100**, 580 (1955).

²E. O. Kane, Phys. Chem. Solids **1**, 249 (1957).

³M. Cardona, J. H. Pollak, and J. G. Broerman, Phys. Lett. **19**, 276 (1965).

⁴N. E. Christensen and M. Cardona, Solid State Commun. **51**, 491 (1984).

⁵R. Eppenga and M. F. H. Schuurmans, Phys. Rev. B **37**, 10923 (1988).

⁶S. S. Nedorezov, Zh. Eksp. Teor. Fiz. **12**, 2276 (1970) [Sov. Phys.—Solid State **12**, 1814 (1971)].

⁷I. Suemune and L. A. Coldren, IEEE J. Quantum Electron. **QE-24**, 1778 (1988).

⁸Walter A. Harrison, *Solid State Theory*, 1st ed. (McGraw-Hill, New York, 1970), Chap. 3, Sec. 5.

⁹Johnson Lee, J. Appl. Phys. **54**, 5482 (1983).